A&A 628, L1 (2019)
https://doi.org/10.1051/0004-6361/201936030

Astronomy & Astrophysics

LETTER TO THE EDITOR

Ross 128 – GL 447

A possible activity cycle for a slow-rotating fully convective star

R. V. Ibañez Bustos[1,2]⋆, A. P. Buccino[1,3], M. Flores[4,5], and P. J. D. Mauas[1,3]

[1] Instituto de Astronomía y Física del Espacio (CONICET-UBA), C.C. 67 Sucursal 28, C1428EHA Buenos Aires, Argentina
e-mail: ribanez@iafe.uba.ar
[2] Departamento de Física. FI, Universidad de Buenos Aires, Buenos Aires, Argentina
[3] Departamento de Física. FCEyN, Universidad de Buenos Aires, Buenos Aires, Argentina
[4] Instituto de Ciencias Astronómicas, de la Tierra y del Espacio (ICATE-CONICET), San Juan, Argentina
[5] Facultad de Ciencias Exactas, Físicas y Naturales, Universidad Nacional de San Juan, San Juan, Argentina

Received 5 June 2019 / Accepted 6 July 2019

ABSTRACT

Context. Long-term chromospheric activity in slow-rotating fully convective stars has scarcely been explored. Ross 128 (Gl 447) is a slow-rotator and inactive dM4 star that has been extensively observed. It hosts the fourth closest extrasolar planet.
Aims. Ross 128 is an ideal target to test dynamo theories in slow-rotating low-mass stars.
Methods. To characterize the magnetic activity of Ross 128, we studied the S_K-indexes derived from CASLEO, HARPS, FEROS, UVES, and X-shooter spectra. Using the generalized Lomb-Scargle and CLEAN periodograms, we analyzed the whole S_K time-series obtained between 2004 and 2018. We performed a similar analysis for the Na I-index, and we analyzed its relation with the S_K-index.
Results. From both indexes, we obtain a possible activity cycle with a period of about five years, which is one of a small handful of activity cycles that have been reported for a slow-rotating fully convective star.

Key words. stars: activity – stars: late-type – techniques: spectroscopic

1. Introduction

Cool main-sequence stars later than M3.5-4V (with masses lower than $\sim 0.35\,M_\odot$) are thought to be fully convective (Chabrier & Baraffe 1997). For decades, many authors therefore assumed that a standard solar-$\alpha\Omega$ dynamo could not operate in these stars due to the absence of a tachocline (Chabrier & Küker 2006; Browning 2008; Reiners & Basri 2010). In this context, Pizzolato et al. (2003) and Wright et al. (2011) studied the X-ray rotation-activity relationship in late-type stars through $L_X/L_{\rm bol}$ versus $P_{\rm rot}$ and $L_X/L_{\rm bol}$ versus $R_{\rm o}$ diagrams. In both diagrams they found two regimes: a saturated and a non-saturated regime. Wright et al. (2011) suggested that this bimodality might be caused by two different dynamos: a convective dynamo parameterized by the bolometric luminosity for fast-rotator stars, and an interface-type dynamo parameterized by the Rossby number for slow rotators ($P_{\rm rot} > 10$ days). However, it was still unclear why two different dynamo configurations would exist in response to two regimes whose transition seemed to be rather smooth. Recently, Wright et al. (2018) extended this analysis by including slow-rotating fully convective stars in the $L_X/L_{\rm bol}$ diagram. The authors concluded that the rotation-activity relationship for fully convective stars (both slow and fast-rotators) present a similar behavior to partly convective stars, as also observed in $\log(R'_{\rm HK})$ (Astudillo-Defru et al. 2017). Moreover, multiwavelength observations of slow-rotator stars confirmed that they have strong magnetic fields (Hawley & Pettersen 1991; Reiners et al. 2009). Three-dimensional dynamo simulations without a tachocline (Browning 2008; Yadav et al. 2015, 2016) also show that it is possible to produce large-scale magnetic fields in stellar convection layers. All these studies suggests that an $\alpha\Omega$ dynamo can operate for slow- and fast-rotator fully convective stars even without a tachocline. The detection of activity cycles in fully convective stars might therefore help to better understand the different dynamos that are at work.

On the other hand, in the last decade, M stars have become favorable targets to search for Earth-like planets in the solar neighborhood because of their low mass and the appreciable star-planet contrast ratio. Around 200 exoplanets have been detected orbiting M-dwarf stars through both transit and radial velocity (RV) methods (Bonfils et al. 2005, 2018; Udry et al. 2007; Mayor et al. 2009; Anglada-Escudé et al. 2013, 2016; Crossfield et al. 2015; Gillon et al. 2017; Dittmann et al. 2017; Díaz et al. 2019). However, it is well known that different magnetic phenomena such as starspots, plages, and activity cycles can induce RV shifts that disturb the detectability of planetary signals (Dumusque et al. 2014). The detection of activity cycles in exostars allows us to distinguish between stellar and planetary signals (Robertson et al. 2013; Carolo et al. 2014; Flores et al. 2018). Several theoretical studies have also addressed the effect of stellar activity on planetary atmospheres and habitability (Cuntz et al. 2000; Ip et al. 2004; Buccino et al. 2006, 2007;

⋆ Based on data obtained at Complejo Astronómico El Leoncito, operated under agreement between the Consejo Nacional de Investigaciones Científicas y Técnicas de la República Argentina and the National Universities of La Plata, Córdoba and San Juan.

Cohen et al. 2010; Dumusque et al. 2017). M-dwarfs stars, with particularly strong flares, are ideal to study these effects.

In the last three years, Earth-like planets orbiting late-type M dwarfs have been reported: Proxima Centauri (M5.5Ve; Anglada-Escudé et al. 2016), TRAPPIST-1 (M8; Gillon et al. 2017), LHS 1140 (M4.5V; Dittmann et al. 2017), and Ross 128 (M4V; Bonfils et al. 2018). In particular, the last three stars are inactive (i.e., they do not emit in Hα). In addition, Proxima Centauri, LHS 1140, and Ross 128 are slow rotators. Of these, activity cycles have only been detected in Proxima Centauri (Cincunegui et al. 2007a; Suárez Mascareño et al. 2016; Wargelin et al. 2017).

To determine the long-term chromospheric activity cycles of late stars, we have developed the HKα Project in 1999. It is dedicated to periodically obtain mid-resolution echelle spectra of fully and partly convective stars. Throughout these 20 years, we have found evidence of cyclic activity in M stars in different regimes: the *fully convective* star Proxima Centauri (Cincunegui et al. 2007a), *partly convective* stars (GJ 229 A and GJ 752 A, Buccino et al. 2011; AU Mic, Ibañez Bustos et al. 2019) and in the *convective threshold* (the binary system GJ 375, Díaz et al. 2007a; AD Leo, Buccino et al. 2014). We also found activity cycles in RS CVn (Buccino & Mauas 2009) and in the K stars ϵ Eri (Metcalfe et al. 2013) and ι Hor (Flores et al. 2017).

In this paper we present a long-term activity study of Ross 128, which has been observed for more than a decade by the HKα Project. This star is a fully convective (M4V) flare star (Lee & Hoxie 1972) with a mass $\sim$0.168 $M_\odot$ and a radius $\sim$0.1967 $R_\odot$. It is a slow rotator with a period of about 121 days. Bonfils et al. (2018) reported a planet orbiting Ross 128 with an orbital period of 9.9 days, which, due to its proximity to the Sun (3.4 parsec), is the fourth closest extrasolar planet. This star is an ideal target to study both the magnetic dynamo in slow-rotating low-mass stars and the impact of stellar activity on planetary atmospheres. We organized this work as follows: in Sect. 2 we present our spectroscopic observations obtained at the Complejo Astronómicómico El Leoncito (CASLEO), which are complemented by public spectroscopic data obtained from the European Southern Observatory (ESO). In Sect. 3 we analyze the decadal time-series in different activity indicators, and finally, we outline our conclusions in Sect. 4.

2. Observations

In 1999 we started the HKα Project to study long-term chromospheric activity in late-type stars (from dF5 to dM5.5). Our database currently contains more than 6000 mid-resolution echelle spectra ($R \approx 13\,000$) covering a wavelength range between 3800 and 6900 Å. These echelle spectra were obtained with the REOSC[1] spectrograph mounted at the 2.15 m *Jorge Sahade* telescope at the CASLEO in San Juan, Argentina. They were optimally extracted and flux calibrated using IRAF[2] procedures (see Cincunegui & Mauas 2004, for details).

In Table 1 we show the observation logs of Ross 128 at CASLEO: 13 individual observations distributed between 2007 and 2018. The first column shows the date (month and year) of the observation, the second column lists xJD = JD − 2 450 000, where JD is the Julian date at the beginning of the observation, and the third column indicates the observing exposure in seconds.

[1] http://www.casleo.gov.ar/instrumental/js-reosc.php

[2] The Image Reduction and Analysis Facility (IRAF) is distributed by the Association of Universities for Research in Astronomy (AURA), Inc., under contract to the National Science Foundation

Table 1. CASLEO spectra for Ross 128 from the HKα project.

Label	xJD	t (s)
0307	4165	7200
0308	4550	7200
0309	4904	7200
0609	4990	5400
0612	6089	5400
0313	6353	7200
0513	6435	7260
0614	6834	5400
0315	7109	5400
0315	7110	6000
0316	7468	5400
0417	7858	6000
0318	8203	6000

Notes. Column 1: Date of each observing run (MMYY). Column 2: Julian date xJD = JD–2450000. Column 3: Exposure time in seconds.

Table 2. ID programs of the Ross 128 observations.

HARPS		FEROS	UVES	X-shooter
072.C-0488(E)	191.C-0873(D)	074.D-0016(A)	091.D-0296(A)	084.D-0795(A)
183.C-0437(A)	191.C-0873(E)	090.A-9003(A)		098.D-0222(A)
191.C-0873(A)	191.C-0873(F)			

We complement our data with public observations obtained with several ESO spectrographs, by the programs listed in Table 2. Forty-one spectra were observed by HARPS, mounted at the 3.6 m telescope ($R \sim 115\,000$), during two time intervals, 2004–2006 and 2012–2016; 3 spectra were obtained in 2005 and 2013 by FEROS, placed on the 2.2 m telescope ($R \sim 48\,000$); 3 spectra were taken in 2013 with UVES, attached to the Unit Telescope 2 (UT2) of the Very Large Telescope (VLT) ($R \sim 80\,000$); and 11 mid-resolution spectra ($R \sim 8900$) were obtained in 2014 and 2017 with X-shooter, mounted at the UT2 Cassegrain focus, in the UVB wavelength range (300–559.5 nm). HARPS and FEROS spectra have been automatically processed by the respective pipelines[3,4]. UVES and X-shooter data were reduced with the corresponding procedure[5,6].

3. Results

3.1. S_K-index

In order to join our dataset with public spectra, which are not calibrated in flux, a dimensionless index for all the spectra is required. For decades, the typical stellar activity indicator used for dF to dK stars has been the Mount Wilson S-index, defined as the ratio of the Ca II- H and K line-core fluxes to the continuum nearby (Baliunas et al. 1998). However, as explained in detail in Buccino et al. (2011), it is not the best index to study the chromospheric activity of the dM4 star Ross 128 because in

[3] http://www.eso.org/sci/facilities/lasilla/instruments/harps.html

[4] http://www.eso.org/sci/facilities/lasilla/instruments/feros.html

[5] http://www.eso.org/sci/facilities/paranal/instruments/uves.html

[6] http://www.eso.org/sci/facilities/paranal/instruments/xshooter.html

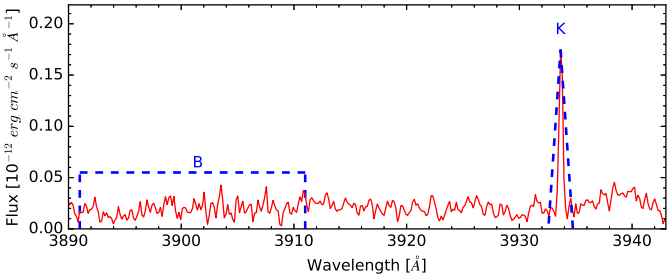

Fig. 1. K line and the blue window for a Ross 128 CASLEO spectrum.

our CASLEO spectra the Ca II-K line presents a greater signal-to-noise ratio than the Ca II-H line. In this work, we use the S_K-index as a proxy of stellar activity. This index is defined as the ratio between the Ca II-K line-core flux integrated with a triangular profile of 1.09 Å FWHM centered in 3933.66 Å and the blue 20 Å window centered at 3901 Å (see Fig. 1).

To corroborate the accuracy of the S_K-index proposed, we computed this index for M-dwarf stars that have previously been studied by our group. We applied a Bayesian analysis to evaluate its correlation with the chromospheric activity indexes reported in Buccino et al. (2011, 2014), and Ibañez Bustos et al. (2019). Using the python code provided by Figueira et al. (2016), we estimated the posterior probability distribution of the correlation coefficient ρ. In all cases, we obtained positive correlation coefficients higher than 0.75[7] with a 95% confidence level.

Before we explored whether this star had an activity cycle, we filtered out any flares from the observations. We visually compared the spectra of nights that were separated by less than a week, and we discarded those with Ca II-K flux higher than 2σ of the mean value. An example is shown in Fig. 2, were we show the Ca II-K, Na I-D1, and the Na I-D2 lines for two close nights with different activity levels. The flare is not only present in the calcium line, but also in the Na lines.

3.2. Long-term activity of Ross 128

In Fig. 3 we show the CASLEO S_K time series compiled for Ross 128 between 2006 and 2018, combined with the S_K-indexes obtained from HARPS, FEROS, UVES, and X-shooter spectra between 2004 and 2017. We intercalibrated the CASLEO, FEROS, UVES, and X-shooter indexes with those of HARPS that were closest in time. We chose the HARPS series as reference because it is the one with both most observations and a wide extension in time. From the whole spectroscopic data series we obtain a variability of $\sigma_{S(K)}/\langle S_K \rangle \sim 25\%$.

Following Ibañez Bustos et al. (2019), we quantified the typical errors of CASLEO spectra by studying the S_K index of the flat star τ Ceti (HD 10700). In this new analysis, we obtained a dispersion of $1\sigma_{S(K)}/\langle S_K \rangle \sim 4\%$ that is coincident with the Mount Wilson index dispersion.

The error bars of HARPS, FEROS, UVES, and X-shooter were obtained in the following way: we grouped the indexes into monthly bins and calculated the standard deviation of each bin. For time intervals with only one index in a month, we adopted the typical RMS dispersion of the bins. In the case of HARPS observations, each point represents the average of two to four nights. The error bars give the idea of the monthly variability of Ross 128, which is higher during its maximum in 2014.

[7] $\rho = (0.750 \pm 0.105)$ for Gl 221A, $\rho = (0.9467 \pm 0.028)$ for Gl 752A, $\rho = (0.859 \pm 0.073)$ for AD Leo and $\rho = (0.825 \pm 0.041)$ for AU Mic.

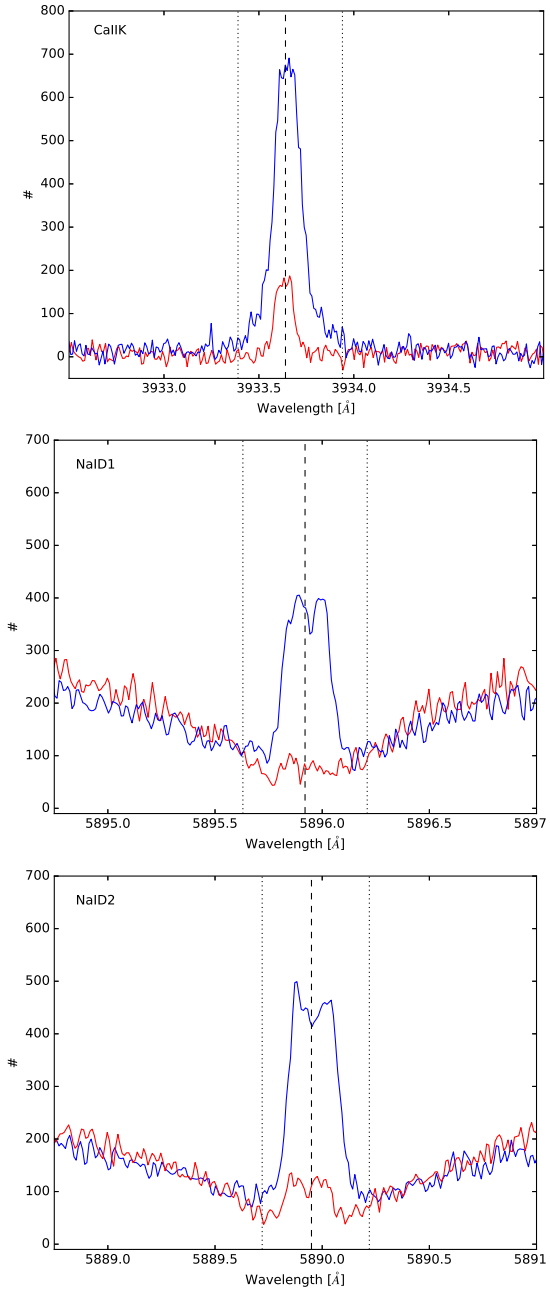

Fig. 2. Ca II- K, Na I D1, and D2 chromospheric lines at different activity levels: flare (blue) and non-flare spectrum (red).

To the whole time series, we computed the generalized Lomb-Scargle (GLS) periodogram (Zechmeister & Kürster 2009) to search for long-term activity cycles (Fig. 4). The periodogram shows two significant peaks at $P = (1956 \pm 98)$ days (~5.4 yr) and $P = (301 \pm 4)$ days (~0.8 year) with very good false-alarm probabilities (FAPs) of 2×10^{-6} and 1×10^{-4}, respectively. The error of the period detected depends on the finite frequency resolution of the periodogram $\delta\nu$ as given by Eq. (2) in Lamm et al. (2004), $\delta P = \frac{\delta\nu P^2}{2}$.

To investigate whether the 301-day period is due to sampling, we implemented the CLEAN deconvolution algorithm described in Roberts et al. (1987). In Fig. 4 we also show the comparison between GLS (blue) and CLEAN (red) periodograms obtained for the whole data. The prominent peak of ~5 yr is present in both the GLS and CLEAN periodograms, but the 301-day

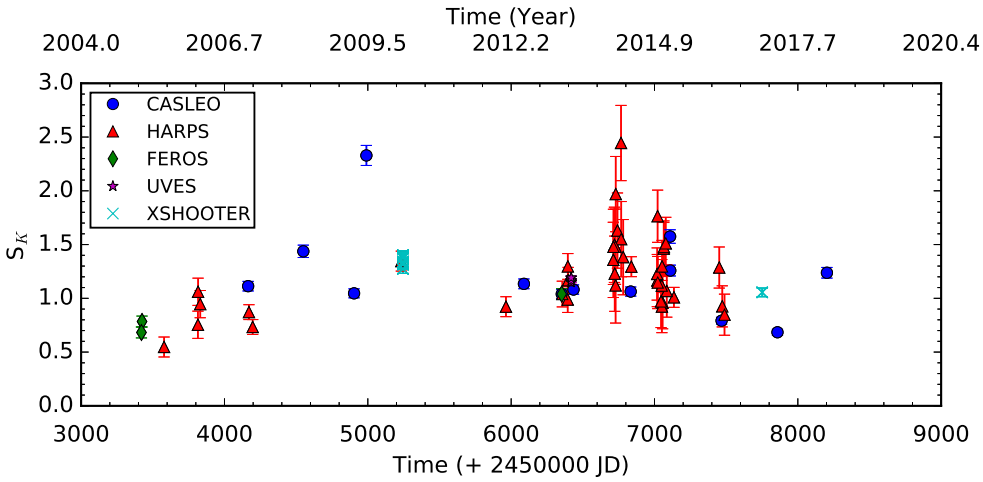

Fig. 3. S_K-indexes for Ross 128 derived from CASLEO (blue filled circle), HARPS (red filled triangle), FEROS ([cmyk]1,0,1,0.4 filled diamond), UVES (violet filled star) and X-shooter (cyan cross) spectra.

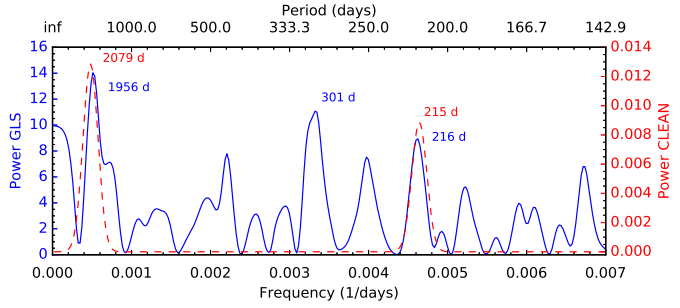

Fig. 4. GLS (blue solid line) and CLEAN (red dashed line) periodograms for the whole S_K time series of Ross 128. There are three prominent peaks for the GLS periodogram: (1956 ± 98) days, (301 ± 4) days, and (216 ± 2) days with FAPs of 2×10^{-6}, 1×10^{-4} , and 2×10^{-3}, respectively.

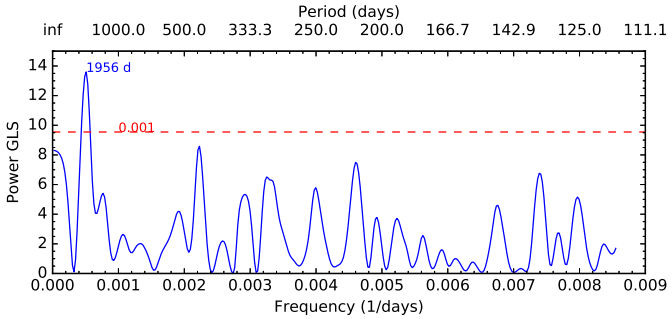

Fig. 5. GLS periodogram after subtracting the ∼109-day period.

period is absent in the CLEAN power spectrum. Therefore this peak is most probably an alias induced by the spectral window function. On the other hand, a 216-day peak is still present in both periodograms, with an FAP of 2×10^{-3} for the GLS method. As this period could be an alias of the 121-day rotation period reported by Bonfils et al. (2018), we estimated the stellar $P_{\rm rot}$ from our activity registry. We first restricted the time series only to spectra with a good signal-to-noise ratio on the Ca II- H line. From these data, we obtained a mean Mount Wilson index $\langle S \rangle = 1.211 \pm 0.230$ and a Ca II- emission level of $\log(R'_{\rm HK}) = -5.621$, both in agreement with the values reported by Astudillo-Defru et al. (2017). Using Eq. (12) of Astudillo-Defru, we obtained a rotation period of ∼109 days, which is nearly half of 216 days. Although the 109-day period is slightly different from the period reported in Bonfils et al. (2018), both are consistent with the stellar activity level. A more exhaustive observation of Ross 128 should be made to determine a reliable rotation period.

We subtracted from our S_K series the modulation with the 109-day rotation period that we found from the previous analysis. For the new residual series, we computed the GLS periodogram, and we found only one prominent peak at ∼5 yr (Fig. 5). Moreover, when we subtracted from our S_K-series the 121-day rotation period reported by Bonfils et al. (2018), the analysis of the residual series was similar to that obtained in Fig. 5. Therefore we discarded the 216-day peak as an activity signal and we conclude that it probably is related to rotational modulation.

3.3. Sodium activity indicators

The spectral range of most of the spectra employed in this analysis enables us to explore activity indicators. In particular, the Na I-D lines provide information about the conditions in the middle to lower chromosphere (Díaz et al. 2007b). For early-M stars, the sodium doublet profiles present extensive wings (more than 20 Å from the line center) and their depth is around 11% of the nearby continuum (Houdebine et al. 2009).

Houdebine et al. (2009) studied the sodium spectral lines for M1 stars. They found a good correlation between the Na I-D1 and D2 line core fluxes, showing that the optical depths decrease with an increasing activity level. This is different from the situation of the Ca II-lines.

M-dwarf stars are usually divided into inactive dM stars, where the Hα line is in absorption, and active dMe stars, which emit in Hα. Using high-resolution HARPS spectra, Gomes da Silva et al. (2012) studied the sodium lines in a sample of low-activity stars with a spectral range from M0 to M3.5 and the late-dMe stars Prox Cen and Barnard's Star. They found that 70% of their sample shows a strong and positive correlation between the Mount Wilson and the sodium indexes.

In this work, we explore the correlation between the Ca II and Na I- lines with only those spectra that include both features. We computed the sodium R'_D-index defined by Gomes da Silva et al. (2012). In Fig. 6 we plot simultaneous measurements of the R'_D-index versus the S_K-index. We found that both indexes are correlated with a Pearson's correlation coefficient of $R = 0.56$. To remove short-term variations due to rotational modulation, we grouped the spectroscopic data every 109 days and found that it remains positive, with a Pearson coefficient of $R = 0.65$

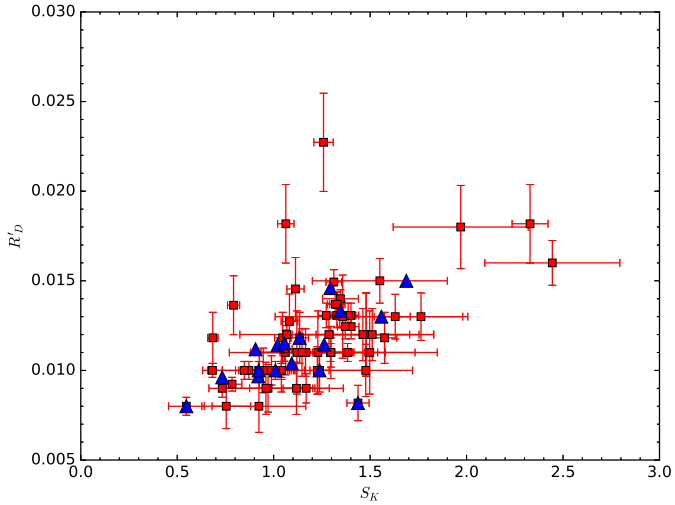

Fig. 6. Simultaneous measurements of the Na I-index R'_D and the S_K-index. The blue triangles indicate the spectroscopic data grouped every 109 days.

for the binned data (blue triangles in Fig. 6). Finally, we built a time series with the R'_D binned indexes and found a period of $P_{\rm Na} = (2151 \pm 285)$ days, similar to the period detected with the S_K series, but with a higher FAP = 0.14, probably related to the long-term activity of Ross 128.

4. Conclusions and summary

The stellar dynamo in fully convective stars has scarcely been explored. In this work, we studied the long-term chromospheric activity of the slow rotator dM4 star Ross 128. We derived the S_K activity index from the Ca II- K line and built for the first time a long time-series employing CASLEO, HARPS, FEROS, UVES, and X-shooter spectra obtained over a span of 14 years. For the whole time series we detected a significant ∼5.4 yr period with both the GLS and CLEAN periodograms. The fact that we obtained this period with both formalisms reinforces the significance of our detection. Furthermore, because most of the spectra that have been collected of Ross 128 cover a wide wavelength range, we were able to study the magnetic activity in the middle chromosphere using the Na I-index. We also detected an activity cycle of $P_{\rm Na} \sim 5.8$ yr with an FAP of 0.14. Moreover, we found a good correlation between the Na I- and the S_K indexes, which remains positive during the whole cycle.

Several cycles have been reported in late-type stars (e.g., Cincunegui et al. 2007b; Buccino et al. 2011; Metcalfe et al. 2013; Ibañez Bustos et al. 2019). However, all these stars belong to the saturation regime in the $L_X/L_{\rm bol}$ versus $P_{\rm rot}/\tau$ diagram (Wright et al. 2011, 2018) and the $\log(R'_{\rm HK})$ versus $P_{\rm rot}$ diagram (Astudillo-Defru et al. 2017). Until now, only one activity cycle of a slow-rotator star was reported in the literature: the active M5.5 star Proxima Centauri (Cincunegui et al. 2007b; Wargelin et al. 2017). Although it has a rotation period of ∼80 days, Prox Cen shows extremely frequent flares and even superflares (Davenport et al. 2016). Its activity level therefore means that this slow-rotator may not belong to the unsaturated regime (Astudillo-Defru et al. 2017).

From our activity register, we obtained a mean activity index $\log R'_{\rm HK} = -5.621$ for Ross 128. If we consider the 121-day rotation period reported by Bonfils et al. (2018), the $\log R'_{\rm HK}$ value place this fully convective M dwarf in the non-saturated regime. From X-ray observations, $L_X/L_{\rm bol} \sim 10^{-5}$ for Ross 128 (Fleming et al. 1995; Malo et al. 2014; Stelzer et al. 2016), which implies that this slow rotator is also outside the saturation regime in the $L_X/L_{\rm bol}$ vs. $P_{\rm rot}$ diagram. On the other hand, in the optical range, Newton et al. (2017) reported a relation between $L_{H\alpha}/L_{\rm bol}$ and the Rossby number, which places Ross 128 in the power-law decay regime. Moreover, the authors found a clear mass-dependent rotation period for inactive stars and estimated a rotation period ∼103 days for this star. This value is in agreement within the statistical error with the value reported by Bonfils et al. (2018) from ASAS photometry and the value that we estimated from the $\log(R'_{\rm HK})$-index.

The activity cycle detected in this work for Ross 128 is in agreement with Wright & Drake (2016), who reported that a solar dynamo could operate in the fully convective stars in the non-saturated regime. In this way, Ross 128 becomes the one of the few slow-rotator stars of its class outside the saturation regime to present a stellar activity cycle.

Likewise, M dwarfs are ideal targets to search for terrestrial planets in the habitable zone. However, stars such as Proxima Centauri (dM5.5e) and TRAPPIST-1 (dM8e) show frequent high-energy flares that could impact on the planetary atmospheres and constrain the habitability of their orbiting planets (Buccino et al. 2006, 2007; Hawley et al. 2014). Recently, Günther et al. (2019) reported that M4-M6 dwarfs are the most common flare stars with 30% of all M stars showing flares. In addition, dM stars (without observable Hα emission activity) are the most abundant in our galaxy. They present flare frequencies much lower than the active ones of the same spectral type, and few of these flares can release high energy (Hawley et al. 2014). Furthermore, Yang et al. (2017) found that the flare activity ($L_{\rm flare}/L_{\rm bol}$) increases as the rotation period decreases, to reach an activity saturation around $\sim 5 \times 10^{-5}$ at periods near ∼5 days. They also suggest that $P_{\rm rot} \sim 10$ days or $L_{\rm flare}/L_{\rm bol} \sim 10^{-6}$ could be a boundary between active and inactive stars. However, at a rotation period longer than 10 days, active stars are mixed with inactive ones. Although flares were also detected in inactive stars, the flare rate and flare energy of inactive and fully convective stars with rotation periods greater than 100 days is not well characterized. Because Ross 128 presents signs of long-term activity, it would be an excellent target for the Transiting Exoplanet Survey Satellite (TESS) to shed light on its flare rate.

References

Anglada-Escudé, G., Tuomi, M., Gerlach, E., et al. 2013, A&A, 556, A126
Anglada-Escudé, G., Amado, P. J., Barnes, J., et al. 2016, Nature, 536, 437
Astudillo-Defru, N., Delfosse, X., Bonfils, X., et al. 2017, A&A, 600, A13
Baliunas, S. L., Donahue, R. A., Soon, W., & Henry, G. W. 1998, ASP Conf. Ser., 154, 153
Bonfils, X., Forveille, T., Delfosse, X., et al. 2005, A&A, 443, L15
Bonfils, X., Astudillo-Defru, N., Díaz, R., et al. 2018, A&A, 613, A25
Browning, M. K. 2008, ApJ, 676, 1262
Buccino, A. P., & Mauas, P. J. D. 2009, A&A, 495, 287
Buccino, A. P., Lemarchand, G. A., & Mauas, P. J. D. 2006, Icarus, 183, 491
Buccino, A. P., Lemarchand, G. A., & Mauas, P. J. D. 2007, Icarus, 192, 582
Buccino, A. P., Díaz, R. F., Luoni, M. L., Abrevaya, X. C., & Mauas, P. J. D. 2011, AJ, 141, 34
Buccino, A. P., Petrucci, R., Jofré, E., & Mauas, P. J. D. 2014, ApJ, 781, L9
Carolo, E., Desidera, S., Gratton, R., et al. 2014, A&A, 567, A48
Chabrier, G., & Baraffe, I. 1997, A&A, 327, 1039
Chabrier, G., & Küker, M. 2006, A&A, 446, 1027
Cincunegui, C., & Mauas, P. J. D. 2004, A&A, 414, 699
Cincunegui, C., Díaz, R. F., & Mauas, P. J. D. 2007a, A&A, 469, 309
Cincunegui, C., Díaz, R. F., & Mauas, P. J. D. 2007b, A&A, 461, 1107
Cohen, O., Drake, J. J., Kashyap, V. L., Sokolov, I. V., & Gombosi, T. I. 2010, ApJ, 723, L64
Crossfield, I. J. M., Petigura, E., Schlieder, J. E., et al. 2015, ApJ, 804, 10

Cuntz, M., Saar, S. H., & Musielak, Z. E. 2000, ApJ, 533, L151
Davenport, J. R. A., Kipping, D. M., Sasselov, D., Matthews, J. M., & Cameron, C. 2016, ApJ, 829, L31
Díaz, R. F., González, J. F., Cincunegui, C., & Mauas, P. J. D. 2007a, A&A, 474, 345
Díaz, R. F., Cincunegui, C., & Mauas, P. J. D. 2007b, MNRAS, 378, 1007
Díaz, R. F., Delfosse, X., Hobson, M. J., et al. 2019, A&A, 625, A17
Dittmann, J. A., Irwin, J. M., Charbonneau, D., et al. 2017, Nature, 544, 333
Dumusque, X., Boisse, I., & Santos, N. C. 2014, ApJ, 796, 132
Dumusque, X., Borsa, F., Damasso, M., et al. 2017, A&A, 598, A133
Figueira, P., Faria, J. P., Adibekyan, V. Z., Oshagh, M., & Santos, N. C. 2016, Origins Life Evol. Biosphere, 46, 385
Fleming, T. A., Schmitt, J. H. M. M., & Giampapa, M. S. 1995, ApJ, 450, 401
Flores, M. G., Buccino, A. P., Saffe, C. E., & Mauas, P. J. D. 2017, MNRAS, 464, 4299
Flores, M., González, J. F., Jaque Arancibia, M., et al. 2018, A&A, 620, A34
Gillon, M., Triaud, A. H. M. J., Demory, B.-O., et al. 2017, Nature, 542, 456
Gomes da Silva, J., Santos, N. C., & Bonfils, X. 2012, A&A, 541, A9
Günther, M. N., Zhan, Z., & Seager, S. 2019, AAS J., submitted [arXiv:1901.00443]
Hawley, S. L., & Pettersen, B. R. 1991, ApJ, 378, 725
Hawley, S. L., Davenport, J. R. A., Kowalski, A. F., et al. 2014, ApJ, 797, 121
Houdebine, E. R., Stempels, H. C., & Oliveira, J. H. 2009, MNRAS, 400, 238
Ibañez Bustos, R. V., Buccino, A. P., Flores, M., et al. 2019, MNRAS, 483, 1159
Ip, W.-H., Kopp, A., & Hu, J.-H. 2004, ApJ, 602, L53
Lamm, M. H., Bailer-Jones, C. A. L., Mundt, R., Herbst, W., & Scholz, A. 2004, A&A, 417, 557
Lee, T. A., & Hoxie, D. T. 1972, Inf. Bull. Variable Stars, 707
Malo, L., Doyon, R., Feiden, G. A., et al. 2014, ApJ, 792, 37
Mayor, M., Bonfils, X., Forveille, T., et al. 2009, A&A, 507, 487
Metcalfe, T. S., Buccino, A. P., Brown, B. P., et al. 2013, ApJ, 763, L26
Newton, E. R., Irwin, J., Charbonneau, D., et al. 2017, ApJ, 834, 85
Pizzolato, N., Maggio, A., Micela, G., Sciortino, S., & Ventura, P. 2003, A&A, 397, 147
Reiners, A., & Basri, G. 2010, ApJ, 710, 924
Reiners, A., Basri, G., & Browning, M. 2009, ApJ, 692, 538
Roberts, D. H., Lehar, J., & Dreher, J. W. 1987, AJ, 93, 968
Robertson, P., Endl, M., Cochran, W. D., & Dodson-Robinson, S. E. 2013, ApJ, 764, 3
Stelzer, B., Damasso, M., Scholz, A., & Matt, S. P. 2016, MNRAS, 463, 1844
Suárez Mascareño, A., Rebolo, R., & González Hernández, J. I. 2016, A&A, 595, A12
Udry, S., Bonfils, X., Delfosse, X., et al. 2007, A&A, 469, L43
Wargelin, B. J., Saar, S. H., Pojmański, G., Drake, J. J., & Kashyap, V. L. 2017, MNRAS, 464, 3281
Wright, N. J., & Drake, J. J. 2016, Nature, 535, 526
Wright, N. J., Drake, J. J., Mamajek, E. E., & Henry, G. W. 2011, ApJ, 743, 48
Wright, N. J., Newton, E. R., Williams, P. K. G., Drake, J. J., & Yadav, R. K. 2018, MNRAS, 479, 2351
Yadav, R. K., Christensen, U. R., Morin, J., et al. 2015, ApJ, 813, L31
Yadav, R. K., Christensen, U. R., Wolk, S. J., & Poppenhaeger, K. 2016, ApJ, 833, L28
Yang, H., Liu, J., Gao, Q., et al. 2017, ApJ, 849, 36
Zechmeister, M., & Kürster, M. 2009, A&A, 496, 577